RSC Advances

ROYAL SOCIETY OF CHEMISTRY

www.rsc.org/advances

Journal Name

RSC Publishing

COMMUNICATION

$Na_{0.56}Ti_{1.72}Fe_{0.28}O_4$: a novel anode material for Na-ion batteries

Cite this: DOI: 10.1039/x0xx00000x

Received 00th January 2012,
Accepted 00th January 2012

DOI: 10.1039/x0xx00000x

www.rsc.org/

Junke Hou[a,b], Yubin Niu[a,b], Wenjun Li[a,b], Fenglian Yi[a,b], Sangui Liu[a,b], Yutao Li[c] and Maowen Xu[a,b*]

A novel $Na_{0.56}Ti_{1.72}Fe_{0.28}O_4$ material is explored as an anode in Na-ion batteries for the first time. It delivers a reversible discharge capacity of 210.3 mA h g^{-1} at 20 mA g^{-1} in Na-ion batteries, exhibiting good capacity retention at a cut-off voltage of 0.01~3 V.

Na-ion batteries have been intensely concerned as a new class of emerging energy storage devices in recent years. Compared with Li-ion batteries, they possess wider resource supplies, lower cost of production and higher system security.[1-2] Such advantages provide a broader development space for Na-ion batteries and accelerate their practical application in the future. In fact, the current research on Na-ion batteries mainly focuses on the electrode materials which can be divided into the cathode and anode. To date, a lot of cathode materials, such as β-$NaMnO_2$,[3] olivine $NaFePO_4$,[4] $Na_3V_2(PO_4)_3$[5] and so on, have been investigated. By contrast, the anode materials for NIBs are limited. Although it is reported that many materials can be used as anode materials for sodium-ion batteries, such as $(Cu_6Sn_5)_{1-x}C_x$,[6] Sb-C,[7] hollow carbon [8], phosphorene,[9] Si,[10-11] and so on. However, the rate performance and cycle life of these materials still need to further improve in the practical application. Thus, it is very necessary to find more alternative anode materials for Na-ion batteries in the future.

In the past few decades, titanate materials have emerged rapidly in the fields of biosensors,[12] adsorbents,[13] photocatalysts,[14] solar cells,[15] supercapacitors,[16] and Li-ion batteries,[17] due to their unique structural channel, one dimensional (1D) nanostructure and large surface area.[18] In fact, the use of titanate as anode material for Na-ion batteries has also been reported in recent years. Among them, $Na_2Ti_3O_7$ shows a suitable capacity of more than 250 mA h g^{-1} at a current density of 354 mA g^{-1} with long service life.[19] $Na_{2.65}Ti_{3.35}Fe_{0.65}O_9$ delivers a capacity of 137.5 mA h g^{-1} at a current rate of 40 mA g^{-1}, which has been reported by our group recently.[20] The monoclinic phase of $Na_4Ti_5O_{12}$ as an anode for Na-ion batteries can obtain a reversible capacity of 64 mA h g^{-1}.[21] Besides, $Na_2Ti_6O_{13}$ displays the ultra-fast (30C or 2min) rate capacity and impressive long cycle life (>5000cycles), but a first discharge capacity is only 65 mA h g^{-1}.[22] Therefore, it is very important to find a new kind of titanate which could improve insertion of Na^+ into per formula units.

Here we used a simple solid-state reaction to synthesize $Na_{0.56}Ti_{1.72}Fe_{0.28}O_4$, and tested its electrochemical performance in Na-ion batteries for the first time. As an anode material for Na-ion batteries, it can deliver a reversible discharge capacity of 210.3 mA h g^{-1} at 20mA g^{-1}, and exhibit a low voltage plateau and long cycle life.

$Na_{0.56}Ti_{1.72}Fe_{0.28}O_4$ sample was synthesized by solid-state reaction of stoichiometric amounts of Na_2CO_3, Fe_2O_3, Fe and TiO_2. The powders were ball-milled for 10 h at 500 rpm, and dried for 12 h at 100 °C. Finally, the obtained powder was heated at 850 °C for 12 h in an Air atmosphere. The anode electrode was prepared by mixing active material, super-P carbon black, and polyvinylidene fluoride (PVdF) in a weight ratio 80: 10: 10 with Nmethyl pyrrolidone (NMP) as solvent. The anode electrodes were pressed onto the copper foil and dried at 120 °C under vacuum for 12 h. The CR2032 coin-type cells consisting of a cathode and sodium metal anode separated by a glass fiber were assembled in a glove box filled with dry argon gas. The electrolyte was 1 M $NaPF_6$ in ethylene carbonate–diethyl carbonate (EC/DEC,

1:1 (v/v)) (Sigma). The galvanostatic charge–discharge tests were performed using a Land battery tester at different rates at 25 °C after 12 h rest.

Powders X-ray diffraction were performed using Cu Kα radiation on a Bruker D8 Advance Diffractometer (XRD, Maxima-X XRD-7000), X-ray photoelectron spectroscopy (XPS) measurements were carried out on a spectrometer (Escalab 250xi, Thermo Scientific) and the morphology of as-prepared materials were also observed using field-emission scanning electron microscopy (FESEM, JSM-6700F) and transmission electron microscopy (TEM, JEM-2100).

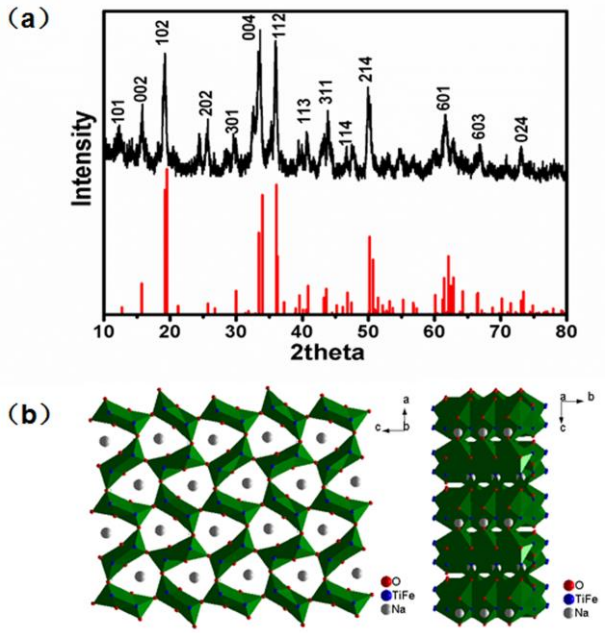

Figure 1 (a) XRD pattern of the as-prepared $Na_{0.56}Ti_{1.72}Fe_{0.28}O_4$ sample; (b) Schematic illustration of the crystal structure of $Na_{0.56}Ti_{1.72}Fe_{0.28}O_4$.

Fig. 1(a) displays the XRD patterns of $Na_{0.56}Ti_{1.72}Fe_{0.28}O_4$. It is clear that the main diffraction peak positions of the obtained materials agree well with $Na_{0.56}Ti_{1.72}Fe_{0.28}O_4$, and the diffraction peaks were assigned to a crystallized orthorhombic structure (space group: *Pnma(62)*). Only trace amounts of impurities existed. Fig. 1(b) schematically shows that the framework of $Na_{0.56}Ti_{1.72}Fe_{0.28}O_4$ is built of $(Fe/Ti)O_6$ octahedral with sharing edges. And we can see the diffusion path of Na^+ is mainly along the b-axis direction for free transport.

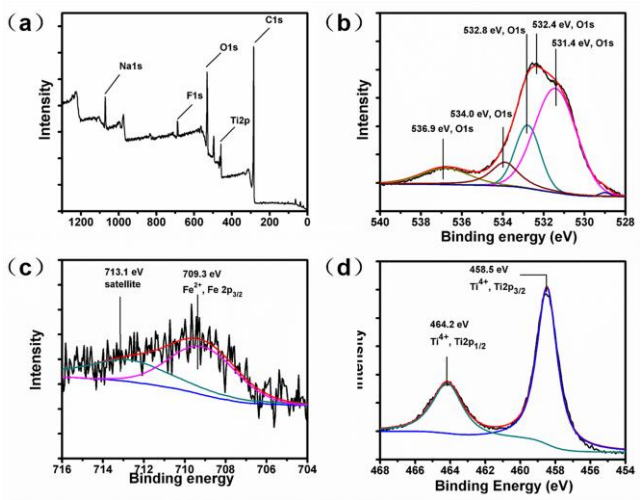

Figure 2 (a) XPS survey spectrum for the surface of $Na_{0.56}Ti_{1.72}Fe_{0.28}O_4$. XPS spectra of (b) O1s (c) Fe 2p and (d) Ti 2p.

The X-ray photoelectron spectroscopy (XPS) was used to investigate the chemical states of Ti, Fe and O. The XPS spectra of $Na_{0.56}Ti_{1.72}Fe_{0.28}O_4$ is displayed in Fig. 2. The wide angle XPS (Fig. 2(a)) of the obtained sample shows the predominant presence of O, Ti, Fe, and Na. From Fig. 2(b), we can see the position of the peaks is 539.9 eV (O^{2-}, O 1s), 534.0 eV (O^{2-}, O 1s), 532.8 eV (O^{2-}, O 1s), 532.4 eV (O^{2-}, O 1s) and 531.4 eV (O^{2-}, O 1s). Fig. 2(c) shows the position of the peak is 709.3 eV (Fe^{2+}, Fe $2p_{3/2}$). And the position of the peaks are 458.5 eV (Ti^{4+}, Ti $2p_{3/2}$) and 464.2 eV (Ti^{4+}, Ti $2p_{1/2}$) from Fig. 2(d).[20, 23] The valence of the Fe, O, Ti is +2, -2 and +4, respectively, which is consistent with the molecular formula.

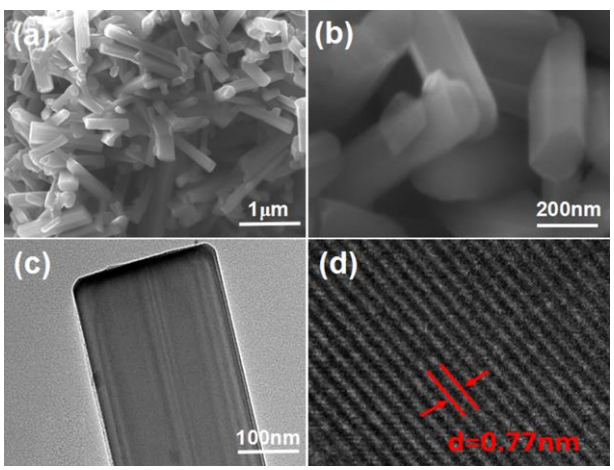

Figure 3 (a, b) SEM images of $Na_{0.56}Ti_{1.72}Fe_{0.28}O_4$ with different magnifications; (c) TEM images of $Na_{0.56}Ti_{1.72}Fe_{0.28}O_4$; (d) High-resolution TEM image of $Na_{0.56}Ti_{1.72}Fe_{0.28}O_4$.

The FESEM and TEM images of the as-prepared $Na_{0.56}Ti_{1.72}Fe_{0.28}O_4$ rods are shown in Fig. 3. Fig. 3(a) is a typical SEM image of $Na_{0.56}Ti_{1.72}Fe_{0.28}O_4$ rods at relatively

low magnification, and the length of uniform rods is 1~2 μm. From the Fig. 3(b), it can be clearly observed that the rods with a diameter of 100~200 nm have been obtained. The width of rods is approximately 200 nm from the TEM image (Fig. 3(c)), while the HRTEM image (Fig. 3(d)) clearly shows lattice fringes indicating single crystallinity of the platelets. The width (0.69 nm) of neighbouring lattice fringes corresponds to the (101) plane of $Na_{0.56}Ti_{1.72}Fe_{0.28}O_4$.

Fig. S1 shows the FESEM images of $Na_{0.56}Ti_{1.72}Fe_{0.28}O_4$ after 20 cycles. From the figure we can see the structure of the material is substantially unchanged. As shown in Fig. S2, the energy-dispersive X-ray (EDX) mapping images of $Na_{0.56}Ti_{1.72}Fe_{0.28}O_4$ show no impurities, and all three elements – Na, Ti, Fe and O are present uniformly throughout the bulk of the sample.

The Na-ion insertion–extraction behavior of $Na_{0.56}Ti_{1.72}Fe_{0.28}O_4$ is studied by galvanostatic charge–discharge test as shown in Fig. 4. The differential specific capacity plots of the 1st, 2nd and 3rd cycle are shown in Fig. 4(a). The first charge–discharge capacity is 217.1/344.5 mA h g^{-1} at a current rate of 20 mA g^{-1}, respectively. The following charge–discharge capacities are 202.5/210.3 mA h g^{-1} and 195.5/202.3 mA h g^{-1} in the 2nd and 3rd cycle, respectively. To understand the electrochemical Na-ion insertion-extraction processes clearly in the first three cycles, cyclic voltammetry studies (CVs) were performed on $Na_{0.56}Ti_{1.72}Fe_{0.28}O_4$, the CVs were conducted in the voltage range 0.01 to 3 V at 0.1 mV s^{-1} and the results are shown in Fig. 4b. The first cycle reduction process consists of three peaks (at 0.766 V, 0.419 V and 0.144 V). On the subsequent cycling, the reduction peaks of 0.766 V and 0.419 V completely vanish. The first cycle oxidation process has four peaks (at 0.089 V, 0.322 V, 0.455 V and 0.768 V), the position of the oxidation peaks were basic unchanged after the subsequent cycling. The CV peaks overlap well for the 2nd and 3rd cycle, which indicates good reversibility of the charge–discharge reactions.

When the cell was charged to 3 V after 20 cycles, the position of peaks are 457.2 eV (Ti^{3+}, Ti $2p_{3/2}$), 458.5 eV (Ti^{4+},Ti $2p_{3/2}$), 463.3 eV (Ti^{3+},Ti $2p_{1/2}$), 464.5 (Ti^{4+},Ti $2p_{1/2}$) and 709.3 eV (Fe^{2+}, Fe $2p_{3/2}$); and when the cell was discharged to 0.01 V after 20 cycles, the position of peaks are 456.8 eV (Ti^{3+}, Ti $2p_{3/2}$), 458.7 eV (Ti^{4+},Ti $2p_{3/2}$), 464.3 eV (Ti^{4+},Ti $2p_{1/2}$) and 706.7 eV (Fe^0, Fe $2p_{3/2}$), 709.1 eV (Fe^{2+}, Fe $2p_{3/2}$) (Fig, S3). According to the reaction mechanism proposed for Fe and Ti in the earlier studies,[19, 24] the capacity are provided by $Ti^{4+} \leftrightarrow Ti^{3+}$ and $Fe^{2+} \leftrightarrow Fe^0$ in this experiment. The electrochemical equation for sodium storage can hence be stated as follows:

$$Na_{0.56}Ti_{1.72}Fe_{0.28}O_4 + 0.56Na^+ + 0.56e^- \leftrightarrow Na_{1.12}Ti_{1.72}O_4 + 0.28Fe \quad (1)$$

$$Na_{0.56}Ti_{1.72}Fe_{0.28}O_4 + 1.72Na^+ + 1.72e^- \leftrightarrow Na_{2.28}Ti_{1.72}Fe_{0.28}O_4 \quad (2)$$

The voltage plateau at approximately 0.766 V, representing the reduction of Fe ions into Fe metal (Fe^0). The other peak at 0.419 V is related to the process of Ti^{4+} transform into Ti^{3+}. Given by Equation 1 (2), respectively.

The cycling stability and the Coulombic efficiency are also displayed in Fig. 4 (c), the capacity is still maintained at 174.6 mA h g^{-1} at a current rate of 20 mA g^{-1} after 100 cycles, and the corresponding capacity retention is 83 %, and the Coulombic efficiency is close to 100% except the first cycle, showing good cycling stability. The rate performance of the $Na_{0.56}Ti_{1.72}Fe_{0.28}O_4$ composite electrode is summarized in Fig. 4 (d). The reversible capacities were 210.2, 171.8, 137.1, 111.2, 90.4, 69.1 and 49.4 mA h g^{-1} at the current rates of 20, 40, 80, 100, 200, 500 and 1000 mA g^{-1}, respectively. Even at the current density of 40 and 20 mA g^{-1} again, a discharge capacity of 133.3 and 166.5 mA h g^{-1} can still be achieved, respectively. The good electrochemical performance of $Na_{0.56}Ti_{1.72}Fe_{0.28}O_4$ cells are mostly attributed to the structure stability of the $Na_{0.56}Ti_{1.72}Fe_{0.28}O_4$ electrode material during Na-ion insertion–extraction processes.[25-26] Therefore, the $Na_{0.56}Ti_{1.72}Fe_{0.28}O_4$ electrode material is promising in practical Na-ion batteries because of its good reversible structure change after Na-ion extraction–insertion processes.

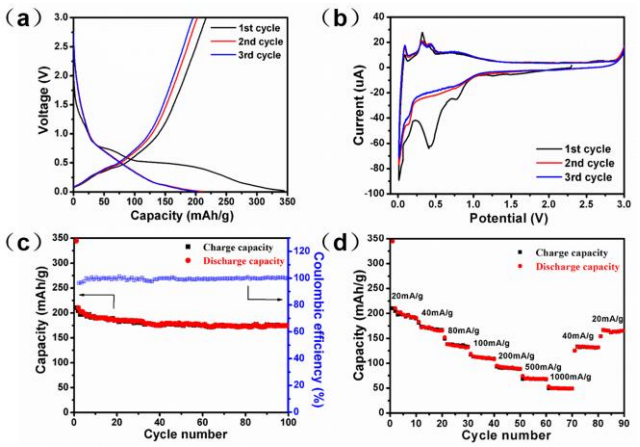

Figure 4 Performance of $Na_{0.56}Ti_{1.72}Fe_{0.28}O_4$. (a) The 1st, 2nd and 3rd charge/discharge curves of $Na_{0.56}Ti_{1.72}Fe_{0.28}O_4$ at a current rate of 20 mA g^{-1} in the voltage range of 0.01 and 3 V versus Na^+/Na; (b) CV curves at a scan rate of 0.1 mV s^{-1} showing the first, the second and the third cycle of the $Na_{0.56}Ti_{1.72}Fe_{0.28}O_4$ composite electrode at a voltage window of 0.01 ~ 3 V; (c) Long-term cycling performance of the $Na_{0.56}Ti_{1.72}Fe_{0.28}O_4$ at a current rate of 20 mA g^{-1} in the voltage range of 0.01 and 3 V versus Na^+/Na; (d) Rate capability of the $Na_{0.56}Ti_{1.72}Fe_{0.28}O_4$. The capacity versus cycle number at various current rates.

In summary, we have synthesized $Na_{0.56}Ti_{1.72}Fe_{0.28}O_4$ by a simple solid-state route. The Na-ion extraction–insertion behavior of $Na_{0.56}Ti_{1.72}Fe_{0.28}O_4$ is investigated in detail for the first time. It delivered a discharge capacity of 210.3 mA h g^{-1} at a current density of 20 mA g^{-1}, and it presents a good capacity and cycle life compared with the aforementioned material. $Na_{0.56}Ti_{1.72}Fe_{0.28}O_4$ holds great promise as an anode material for Na-ion batteries applications.

Acknowledgements

This work is financially supported by Chongqing Key Laboratory for Advanced Materials and Technologies of Clean Energies under cstc2011pt-sy90001, Start-up grant under SWU111071 from Southwest University and Chongqing Science and Technology Commission under cstc2012gjhz90002 and cstc2015jcyjA50031. The work is supported by grants from Fundamental Research Funds for the Central Universities (SWU113079, XDJK2014C051).

Notes and references

[a]*Institute for Clean Energy & Advanced Materials, Faculty of Materials and Energy， Southwest University, Chongqing 400715, P.R. China*
[b]*Chongqing Key Laboratory for Advanced Materials and Technologies of Clean Energies, Chongqing 400715, P.R. China*
[c]*Texas Materials Institute, University of Texas at Austin, Texas 78712, USA*
Fax: +86-23-68254969; Tel: +86-23-68254969;
E-mail: xumaowen@swu.edu.cn

1 D. A. Stevens and J. R. Dahn, *J. Electrochem. Soc.*, 2000, **147**, 1271.
2 M. D. Slater, D. Kim, E. Lee, M. M. Doeff and C. S. Johnson, *Adv. Funct. Mater.*, 2013, **23**, 947.
3 J. Billaud, R. J. Cle ´ment, A. R. Armstrong, J. C. Va ´zquez, P. Rozier, C. P. Grey and P. G. Bruce, *J. Am. Chem. Soc.*, 2014, **136**, 17243.
4 K. Zaghib, J. Trottier, P. Hovington, F. Brochu, A. Guerfi, A. Mauger and C. Julien, *J. Power Sources*, 2011, **196**, 9612.
5 Z. Jian, W. Han, X. Lu, H. Yang, Y. Hu, J. Zhou, Z. Zhou, J. Li, W. Chen, D. Chen and L. Chen, *Adv. Energy Mater.*, 2013, **3**, 156.
6 J. S. Thorne, R. A. Dunlap and M. N. Obrovac, *Electrochim. Acta*, 2013, **112**, 133.
7 L. Wu, X. Hu, J. Qian, F. Pei, F. Wu, R. Mao, X. Ai, H. Yang and Y. Cao, *Energy Environ. Sci.*, 2014, **7**, 323.
8 Y. Cao, L. Xiao, M. L. Sushko,W.Wang, B. Schwenzer, J. Xiao, Z. Nie, L. V. Saraf, Z. Yang and J. Liu, *Nano Lett.*, 2012, **12**, 3783.
9 V. V. Kulish, O. I. Malyi, C. Persson and P. Wu, *Phys. Chem. Chem. Phys.*, 2015, **17**, 13921.
10 O. Malyi, V. V. Kulish, T. L. Tan, S. Manzhos, *Nano Energy*, 2013, **2**, 1149.
11 S. Komaba, Y. Matsuura, T. Ishikawa, N. Yabuuchi, W. Murata, S. Kuze, *Electrochem. Commun.*, 2012, **21**, 65.
12 A. Liu, M. Wei, I. Honma and H. Zhou, *Adv. Funct. Mater.*, 2006, **16**,371.
13 Q. Deng, C. Huang, H. Xu and M. Wei, *Nanoscale*, 2013, **5**, 5519.
14 Y. Ide, Y. Nakasato and M. Ogawa, *J. Am. Chem. Soc.*, 2010, **132**, 3601.
15 A. Pang, L. Xia, H. Luo and M. Wei, *Electrochim. Acta*, 2013, **94**, 92.
16 Y. Wang, Z. Hong, M. Weiand Y. Xia, *Adv. Funct. Mater.*, 2012, 22, 5185.
17 J. R. Li, Z. Tang and Z. Zhang, *Chem. Mater.*, 2005, **17**, 5848.
18 J. Yang, L. Lian, P. Xiong and M. Wei, *Chem. Commun.*, 2014, **50**, 5973.
19 W. Wang, C. Yu, Z. Lin, J. Hou, H. Zhu and S. Jiao, *Nanoscale*, 2013, **5**, 594.
20 M. Xu, J.-K. Hou, Y.-B. Niu, G.-N. Li, Y.-T. Li and C. M. Li, *Chem. Commun.*, 2015, **51**, 3227.
21 P. Naeyaert, M. Avdeev, N. Sharma, H. Yahia and C. Ling, *Chem. Mater.*, 2014, **26**, 7067.
22 A. Rudola, K. Saravanan, S. Devaraj, H. Gong and P. Balaya, *Chem. Commun.*, 2013, **49**, 7451.
23 G. K. Mor, H. E. Prakasam, O. K. Varghese, K. Shankar and C. A. Grimes, *Nano Lett.*, 2007, ***7* (8)**, 2356.
24 M. V. Reddy, T. Yu, C.-H. Sow, Z. X. Shen, C. T. Lim, G. V. S. Rao and B. V. Chowdari, *Adv. Funct. Mater.*, 2007, **17**, 2792.
25 J. Wang, B. Qiu, X. He, T. Risthaus, H. Liu, M. C. Stan, S. Schulze, Y. Xia, Z. Liu, M. Winter and J. Li, *Chem. Mater.*, 2015, **27**, 4374.
26 J. S. Thorne, S. Chowdhury, R. A. Dunlap, and M. N. Obrovac, *J Electrochem. Soc.*, 2014, **161** (12), A1801.